On the Air–Sea Boundary in Transient Marine CSEM Detection Modeling of Subseafloor Hydrocarbon Reservoirs

Jiajun Niu, *Student Member, IEEE*, and Jamesina J. Simpson, *Member, IEEE*

***Abstract*—The published scientific literature provides extensive results and discussion of approximate finite-difference time-domain (FDTD) computational modeling of marine controlled-source electromagnetics (CSEM) detection of hydrocarbon reservoirs buried under the seafloor. "Approximate" here refers to the neglection of displacement currents in the calculation to reduce the computational burden of the simulation. This leads to the widely used approximate continuation boundary conditions at the ocean–air interface to avoid the free-space region in the simulation where inclusion of displacement currents is required. However, an analysis of when the use of such continuation boundary conditions sufficiently reduces the accuracy of the calculated results is lacking in the published literature. This letter addresses this issue and reports the application of the complete and standard, three-dimensional full-vector Maxwell's equations FDTD method to modeling CSEM hydrocarbon detection. We provide accurate results for shallow and deep-water CSEM problems and determine that the continuation boundary condition is inadequate at large (> 4.5 km) source-to-receiver distances in deep-water detection problems and at all distances in shallow-water problems.**

***Index Terms*—Airwave, finite-difference time domain (FDTD), marine controlled-source electromagnetics (CSEM), subseafloor hydrocarbon reservoir, transient marine controlled-source electromagnetics (tCSEM).**

I. Introduction

THE MARINE controlled-source electromagnetics (CSEM) method is an effective tool for subseafloor hydrocarbon exploration under deep seawater [1], [2]. However, as the depth of the seawater decreases to less than $\sim$300 m, the returned airwave (the coupling and reflections generated at the air–seawater interface) begins to dominate over the reservoir response at the seafloor receivers [3]. This effect creates a challenge for the conventional frequency CSEM (fCSEM) method in detecting thin resistive reservoirs under shallow seawater, and is often called the shallow-water problem [4]. To overcome this problem, Weiss [4] suggests the use of the transient CSEM (tCSEM) method introduced by Edwards [5] and demonstrated by other groups [6], [7]. According to Weiss [4], the shallow-water problem is "one in which accurate simulation of atmospheric coupling is required."

Following the development of analytical formulations [8] for half-space problems, several time-domain finite-difference (FD) methods have been developed and applied to simulating low-frequency three-dimensional (3-D) geological problems [9]–[11]. These methods, which are based on a diffusive approximation, are designed to reduce the computation time. Therefore, none of them employ the standard full-vector Maxwell's equations finite-difference time-domain (FDTD) method [12], and thus none model propagation in the air region. Instead, these techniques involve either an approximate upward continuation boundary condition, and/or an artificially high permittivity in order to permit a larger FD time-step (thereby reducing the total simulation time) [9], or a transformation method [10] that yields realistic frequency-domain electromagnetic fields but nonphysical time-domain solutions [11].

In this letter, we report the application of the 3-D full-vector Maxwell's equations FDTD method [12] to marine CSEM modeling. The complete FDTD method is chosen here in order to provide accurate calculations that include the atmospheric coupling and propagation in the air region above the ocean surface. Thus, realistic electromagnetic parameters are simulated, instead of artificially high values, and a small time-step governed by the standard FDTD Courant limit is employed. As a result, however, the model is computationally expensive. This tradeoff for accuracy is made so that the appropriateness of the ocean–air boundary in traditional (approximate, but more efficient) CSEM calculations may be evaluated.

Recently, one conference publication [13] has appeared wherein the full-vector FDTD method is applied to CSEM hydrocarbon exploration. The goal in [13] is to develop an efficient means of including the airwave via a total field scattered field formulation. Their methodology involves first a single full-vector FDTD simulation with no hydrocarbon reservoir present in order to obtain the airwave due to the source and background geometry (sediment, ocean, and air). This is followed by any number of simulations using the approximate FDTD method. The motivation behind the work in [13] is that for shallow-water environments, "the effect of the air can no longer be neglected."

Compared to [13], in this letter we use the full-vector FDTD method to demonstrate that at sufficiently large distances from the source, the airwave cannot be neglected for even deep-water frequency-domain problems, as is commonly believed, and that the widely used continuation boundary condition at the

Manuscript received February 16, 2012; revised April 16, 2012; accepted May 16, 2012. Date of publication June 06, 2012; date of current version June 21, 2012.

J. Niu is with the Electrical and Computer Engineering Department, University of New Mexico, Albuquerque, NM 87131 USA.

J. J. Simpson is with the Electrical and Computer Engineering Department, University of Utah, Salt Lake City, UT 84112 USA (e-mail: simpson@ece.utah.edu).

Digital Object Identifier 10.1109/LAWP.2012.2203329

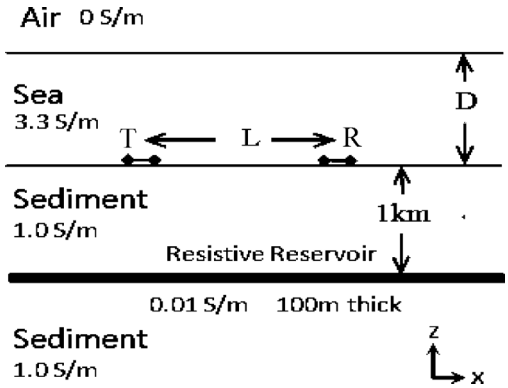

Fig. 1. Canonical 1-D problem.

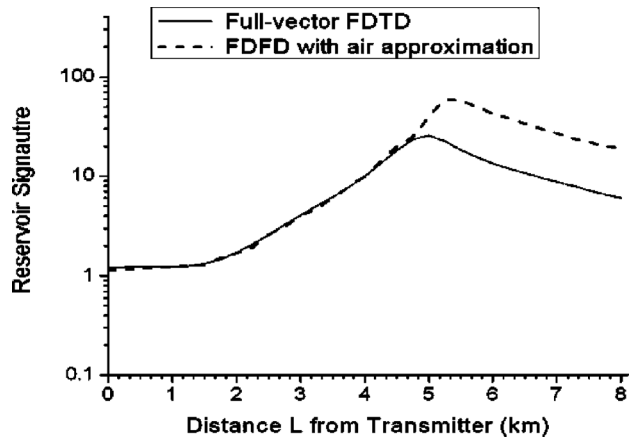

Fig. 2. Reservoir signature with respect to L for the 1-D deep-water fCSEM problem as calculated by 3-D FDTD (solid line) and by FDFD (dashed line) [3].

ocean–air interface in approximate formulations provides inaccurate results at large (> 4.5 km) distances from the source. Furthermore, we demonstrate that the continuation boundary condition provides inaccurate results for shallow-water problems at all distances from the source. Note that the accuracy of the continuation boundary condition has not previously been reported, particularly for large distances from the source in deep-water problems.

II. 3-D Full-Vector FDTD Model

To simulate both wave propagation and diffusion in CSEM surveys, we employ the standard FDTD method [12] based on the full-vector time-domain Maxwell's curl equations.

CPML [12], [15] is incorporated into the FDTD model to prevent unwanted reflections from the outer grid boundaries. Typical reflection errors for CPML are on the order of 1/100 of 1%. Note that for linear media, the implementation of CPML is independent of the materials being terminated by the CPML [15]. This permits the CPML on all sides of the FDTD CSEM model to be implemented identically, regardless of whether air, rock, seawater, reservoir, or any combination of these media is being terminated. Complete Maxwell's equations solutions are obtained at all material interfaces, and no approximate boundary conditions are employed.

In all of the full-vector FDTD simulations, the space increment in each Cartesian direction is set to 50 m, i.e., $\Delta x = \Delta y = \Delta z = 50$ m. The time increment Δt is set to about 1E-7 s, which satisfies the Courant condition. Finally, the 3-D full-vector FDTD CSEM models are implemented on the supercomputer Encanto [16] using message-passing interface (MPI) [17].

III. Simulation Results

We first compare the full-vector FDTD results with frequency-domain FD (FDFD) method [3] calculations for both canonical deep and shallow fCSEM problems. A 1-Hz sinusoidal source excitation is employed. The geometry for the one-dimensional (1-D) geometry canonical problem is shown in Fig. 1. T denotes the transmitter, and R the receiver. L is the distance between the receiver and transmitter, and D is the seawater depth. The conductivity values used to model the air, sea, sediment, and hydrocarbon reservoir are listed in Fig. 1. D is set to either 1 km (deep-water problem) or 300 m (shallow-water problem).

For the deep-water full-vector FDTD simulations, the computational domain comprises 240 cells in the x-direction, 120 cells in the y-direction, and 92 cells in the z-direction. Then, for the shallow-water full-vector FDTD simulations, the domain size is $240 \times 120 \times 80$ cells. The transmitter is modeled as a 200-m-long current source along a series of four cells of the grid and is oriented in the x-direction. Each FDTD model is run on 288 processing cores of the supercomputer Encanto, with the deep-water model running 1.4E8 time-steps in 48 h, and the shallow-water model running 1.5E8 time-steps in 45 h.

A. Canonical 1-D Problem Results

Fig. 2 graphs on a log scale the normalized $|E_x|$ reservoir signature as a function of L for the case of the canonical 1-D deep-water fCSEM problem. To obtain the reservoir signature from the full-vector FDTD model, the fields of E_x (inline with the source) recorded in the time domain are first transformed into the frequency domain through a discrete Fourier transformation (DFT). Then, the reservoir signature is found by dividing the frequency-domain $|E_x|$ at 1 Hz for the case wherein the reservoir is present by the $|E_x|$ for the case wherein there is no reservoir (background case).

Comparing in Fig. 2 the FDTD results with the FDFD results as published in [3], we note the results are nearly identical for observation distances of less than 4.5 km. For distances greater than 4.5 km, the FDTD model includes displacement currents by solving the full-vector Maxwell's equations, and thus provides a robust calculation of the electromagnetic waves propagating in the atmosphere above the ocean surface. On the other hand, the FDFD model neglects displacement currents and replaces the air region with an approximate boundary condition [3]. As a result, since air waves can propagate over larger distances from the source with less attenuation than the waves propagating in the conductive ocean and sediment layers, the difference between the normalized magnitudes at points far from the transmitter (> 4.5 km) between the FDTD and FDFD results is due to the FDFD model neglecting displacement currents, not providing

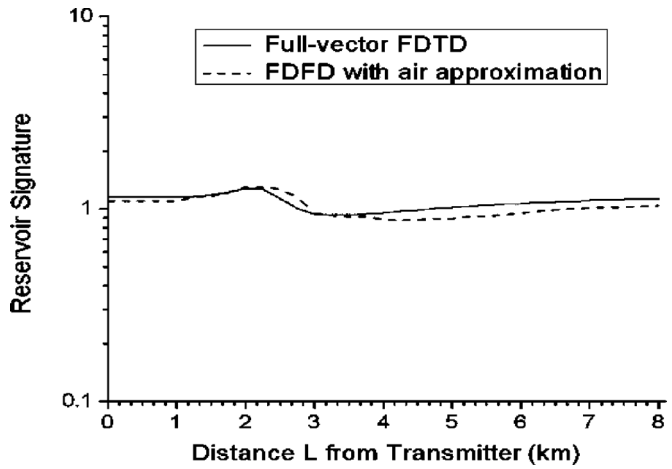

Fig. 3. Reservoir signature with respect to L for the 1-D shallow-water fCSEM problem as calculated by 3-D FDTD (solid line) and by FDFD (dashed line) [3].

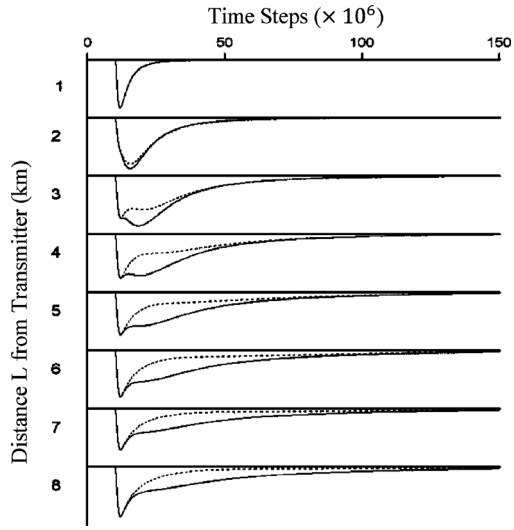

Fig. 4. tCSEM snapshot results of the inline for the 1-D shallow-water problem for the case wherein the reservoir is present (solid line) and the case wherein there is no reservoir (dashed line).

a complete solution to Maxwell's equations for wave propagation in the air region, and instead employing the approximate continuation boundary condition. As a result, the FDFD calculation overestimates the reservoir signature at large distances (> 4.5 km).

Next, Fig. 3 plots the inline normalized $|E_x|$ reservoir signature as a function of L for a 1-D shallow-water fCSEM problem. As for Fig. 2, the full-vector FDTD-calculated signature is found by transforming time-domain data into the frequency domain through a DFT. The two lines representing the FDTD and FDFD results in Fig. 3 show the same general trend. However, there are notable differences due again to the different treatment in modeling the air region. These differences are more pronounced at shorter distances from the source for the shallow-water problem than for the previous deep-water problem since the air region is closer to the transmitter and receivers. The FDFD results of Fig. 3 were previously reported in [3].

Finally, note that there are no significant differences between the unity line representing a normalized field $= 1$ and either the FDTD or FDFD lines in Fig. 3, i.e., the response for the case wherein the reservoir is present is almost identical to that of the background case without the reservoir at all receiving distances from the transmitter. This indicates that traditional fCSEM employing a sinusoidal source is not effective for shallow-water detection problems. In fact, Weiss [4] states that "the existence of a shallow-water problem is an unfortunate result of conventional, frequency-domain survey design."

Instead, tCSEM works better for shallow-water detection problems by employing a time-domain pulse as the source instead of a single-frequency sinusoid. To simulate the reservoir detection via tCSEM, we next choose a Gaussian pulse as the source excitation in the full-vector 3-D FDTD model and calculate the electric field responses in time at various observation points. The Gaussian pulse has a time delay about 1 s and a half-width about 0.1 s. Note that tCSEM, as well as the FDTD model, could employ any arbitrary shaped pulse. Fig. 4 compares the observed E_x time waveforms at varying distances from the transmitter for the canonical 1-D shallow-water tCSEM problems with and without the reservoir using a Gaussian pulse source as calculated by the full-vector FDTD model.

At distances of more than 3 km from the transmitter, it is observed in Fig. 4 that the peak of the airwave arrives earlier than the response of the reservoir. Note that the early-arrival peak generated by the air region has no information about the potential reservoir, while the late-arrival "reservoir" response contains useful information for determining the presence and characteristics of the reservoir. This suggests that it would be useful to separate the "reservoir" response from the early-arrival airwave to aid the detection and characterization of the reservoir. This is in fact the basic principle of shallow-water tCSEM [4]. However, it is important to note that an accurate calculation of the airwave is necessary in order to permit an accurate separation of the "reservoir" response from the early-arrival airwave. As such, care must be taken when employing the continuation boundary condition at the ocean–air interface for shallow-water problems. Conversely, when computationally feasible, the full-vector Maxwell's equation FDTD method should be instead employed as it is here to provide more accurate calculations at the ocean–air interface and of wave propagation, including displacement currents, in the overlying air region.

B. Canonical 3-D Square Disk Problem

As a final demonstration, we take full advantage of the 3-D nature of the full-vector FDTD model by simulating a 3-D geometry shallow-water tCSEM problem (no longer a 1-D geometry problem). The reservoir is no longer represented by an infinite resistive layer, but instead by a finite-dimension square disk. The dimensions of the square disk are 5, 4, and 0.1 km in the x-, y-, and z-directions, respectively. The same Gaussian pulse is chosen as the transmitter excitation in the FDTD simulation. The transmitter is placed over the left edge of the square disk at the midpoint of the disk in the y-direction.

Fig. 5 compares the observed E_x time waveforms at varying distances from the transmitter for the 3-D shallow-water tCSEM

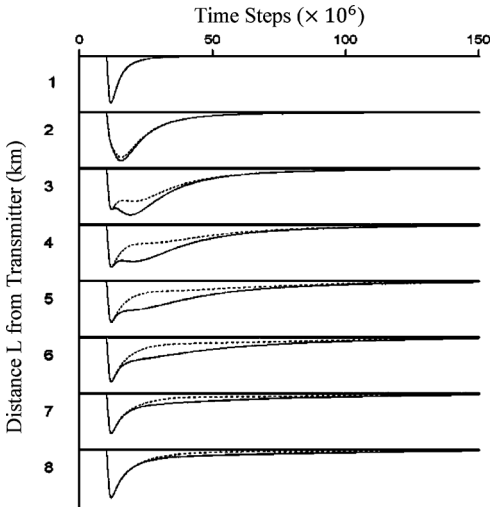

Fig. 5. tCSEM snapshot results of the inline for the 3-D shallow-water problem for the case wherein the reservoir is present (solid line) and the case wherein there is no reservoir (dashed line).

problem for the case wherein the disk reservoir is present with the case wherein there is no disk reservoir. As in Fig. 4, it is also observed in Fig. 5 that the peak of the airwave arrives earlier than the response of the reservoir at distances of more than 3 km from the source. Thus, the "reservoir" response may be separated from the early-arrival airwave in this 3-D problem, provided that the airwave is calculated accurately. Also comparing Fig. 5 to Fig. 4, in Fig. 5 the observed responses for with and without the reservoir at more distant observation points ($L > 5$ km) are much closer in agreement than the corresponding curves in Fig. 4. This is because the distant observation points in Fig. 5 are outside the region of the reservoir disk, where the reflection from the reservoir is weak [18]. However, this implies that an accurate calculation of the airwave is even more important for shallow-water problems involving (more realistic) finite-sized reservoirs than for infinite reservoirs so that details on the location and extent of the reservoir can be accurately extracted from the weak reservoir signal.

IV. Conclusion and Ongoing Work

This letter reported the application of the 3-D full-vector FDTD method to investigating the importance of accurate modeling of the overlying air region and at the ocean–air interface in CSEM hydrocarbon detection problems. In particular, the accuracy of the widely used continuous boundary condition at the ocean–air interface was studied. The complete Maxwell's equations FDTD method was employed in this study to provide robust calculations including the atmospheric coupling and propagation in the air region at the cost of computation time.

The full-vector FDTD model was first verified by comparing its results to published FDFD results in the literature for fCSEM surveys employing a sinusoidal source. The FDTD-calculated results demonstrated that at sufficiently large distances from the source, the airwave cannot be neglected for even deep-water frequency-domain problems, as has been previously believed. Furthermore, the FDTD-calculated results demonstrated that the widely used continuation boundary condition at the ocean–air interface in approximate formulations provides inaccurate results at large (> 4.5 km) distances from the source. Additionally, it was demonstrated that the continuation boundary condition provides inaccurate results for shallow-water problems at all distances from the source. These results are of practical importance for CSEM hydrocarbon detection modeling.

References

[1] S. Constable, "Marine electromagnetic methods – A new tool for offshore exploration," *Leading Edge*, vol. 25, no. 4, pp. 438–444, Apr. 2006.

[2] S. Constable and L. J. Srnka, "An introduction to marine controlled-source electromagnetic methods for hydrocarbon exploration," *Geophysics*, vol. 72, no. 2, pp. WA3–WA12, Mar. 2007.

[3] E. S. Um and D. L. Alumbaugh, "On the physics of the marine controlled-source electromagnetic method," *Geophysics*, vol. 72, no. 2, pp. WA13–WA26, Mar. 2007.

[4] C. J. Weiss, "The fallacy of the 'shallow-water problem' in marine CSEM exploration," *Geophysics*, vol. 72, no. 6, pp. A93–A97, Nov. 2007.

[5] R. N. Edwards, "On the resource evaluation of marine gas hydrate deposits using the sea-floor transient electric dipole-dipole method," *Geophysics*, vol. 62, no. 1, pp. 63–74, Jan. 1997.

[6] N. Allegar, K. Strack, R. Mittet, and A. Petrov, "Marine time domain CSEM—The first two years of experience," in *Proc. 70th EAGE Conf. Exhib.*, Rome, Italy, Jun. 2008, pp. 9–12.

[7] A. Ziolkowski, "CSEM data in shallow water," in *Proc. EGM Int. Workshop*, Capri, Italy, Apr. 2010, pp. 1–4.

[8] R. W. P. King, "The electromagnetic field of a horizontal electric dipole in the presence of a three-layered region," *J. Appl. Phys.*, vol. 69, pp. 7987–7995, Jun. 1991.

[9] T. Wang and G. W. Hohmann, "A finite-difference, time-domain solution for three-dimensional electromagnetic modeling," *Geophysics*, vol. 58, no. 6, pp. 797–809, Jun. 1993.

[10] F. A. Maaø, "Fast finite-difference time-domain modeling for marine-subsurface electromagnetic problems," *Geophysics*, vol. 72, no. 2, pp. A19–A23, Mar. 2007.

[11] R. Mittet, "High-order finite-difference simulations of marine CSEM surveys using a correspondence principle for wave and diffusion fields," *Geophysics*, vol. 75, no. 1, pp. F33–F50, Jan. 2010.

[12] A. Taflove and S. C. Hagness, *Computational Electrodynamics: The Finite-Difference Time-Domain Method*, 3rd ed. Norwood, MA: Artech House, 2005.

[13] A. Dukeshire, T. Tan, M. Okoniewski, and M. Potter, "Marine CSEM scattered subsurface response detection using total-field scattered-field FDTD formulation," in *Proc. 5th EuCAP*, 2011, pp. 1367–1370.

[14] A. H. Bhuyian, B. P. Thrane, M. Landrø, and S. E. Johansen, "Controlled source electromagnetic three-dimensional grid-modelling based on a complex resistivity structure of the seafloor: Effects of acquisition parameters and geometry of multi-layered resistors," *Geophys. Prospecting*, vol. 58, no. 3, pp. 505–533, May 2010.

[15] J. A. Roden and S. D. Gedney, "Convolution PML (CPML): An efficient FDTD implementation of the CFS-PML for arbitrary media," *Microw. Opt. Technol. Lett.*, vol. 27, no. 5, pp. 334–339, Dec. 2000.

[16] New Mexico Computing Applications Center, Albuquerque, NM, "Encanto—New Mexico's supercomputer," 2012 [Online]. Available: http://nmcac.net/encanto.html

[17] C. Guiffaut and K. Mahdoubi, "A parallel FDTD algorithm using MPI library," *IEEE Antennas Propag. Mag.*, vol. 43, no. 2, pp. 94–103, Apr. 2001.

[18] S. Constable and C. J. Weiss, "Mapping thin resistors and hydrocarbons with marine EM methods: Insights from 1D modeling," *Geophysics*, vol. 71, no. 2, pp. G43–G51, Mar. 2006.